

The 1966 'century' flood in Italy: a meteorological and hydrological revisitation

P. Malguzzi \*, G. Grossi\*\*,  
A. Buzzi \*, R. Ranzi\*\*, R. Buizza

Research Department

\*ISAC-CNR, Bologna; \*\*Univ. of Brescia

July 2006

Submitted for publication in J. Geoph. Research.

This paper has not been published and should be regarded as an Internal Report from ECMWF.  
Permission to quote from it should be obtained from the ECMWF.



**Series: ECMWF Technical Memoranda**

A full list of ECMWF Publications can be found on our web site under:  
<http://www.ecmwf.int/publications.html>

[library@ecmwf.int](mailto:library@ecmwf.int)

**© Copyright 2006**

European Centre for Medium Range Weather Forecasts  
Shinfield Park, Reading, Berkshire RG2 9AX, England

Literary and scientific copyrights belong to ECMWF and are reserved in all countries. This publication is not to be reprinted or translated in whole or in part without the written permission of the Director. Appropriate non-commercial use will normally be granted under the condition that reference is made to ECMWF.

The information within this publication is given in good faith and considered to be true, but ECMWF accepts no liability for error, omission and for loss or damage arising from its use.

## Abstract

The widespread flood event that affected north-eastern and central Italy in November 1966, causing severe damages to vast populated areas including the historical towns of Florence and Venice, is revisited with a modelling approach, made possible by the availability of the ECMWF global reanalysis (ERA-40). A simulated forecasting chain consisting of the ECMWF global model, forcing a cascade of two mesoscale, limited-area meteorological models apt to reach a convective resolving scale (about 2 km), is used to predict quantitative precipitation. A hydrological model, nested in the finer-scale meteorological model, is used to reproduce forecasted flood hydrographs for different river basins of the investigated areas. Predicted precipitation is in general very sensitive to initial conditions, especially when associated with convective activity, such as over central Italy, in the Arno river basin. Orographically enhanced precipitation, e.g. the one predicted in the eastern Alps, is quite stable and in good agreement with observations. Hydrological forecasts, made separately in different river basins, reflect the accuracy of the simulated precipitation.

## 1. Introduction

In the period from 3 to 5 November 1966, central and north-eastern Italy was affected by a synoptic scale, severe cyclonic system that caused catastrophic and widespread damages associated with flooding, storm surges and landslides. The most memorable effects were the Arno river flooding in Florence that caused severe losses of artistic heritage, the extreme high water in Venice, and the flooding of the town of Trento (geographical locations are shown in Figure 2, 4, and 8). However, damages and casualties due to flooding and landslides were reported in several areas, including the eastern Alps where the heaviest precipitation was observed.

In Tuscany (see Figure 8), the rainfall event was extreme in terms of continuity, intensity, and area coverage (Ministero dei Lavori Pubblici, 1970). The temporal and spatial distribution of precipitation was considered as the “worst possible” from the point of view of the hydrological response of the Arno river basin (De Angelis, 1969). Precipitation started around noon of 3 November. During the following night, the Arno water level increased by several meters (six meters in six hours) until the levees were overtopped and broken in different sites. The water reached the Cathedral Square in Florence at around 10 a.m. local time of the following day. In the Arno watershed, highways and railroads were submerged. Only in the evening of 4 November the river water level started to decrease.

Several papers have been published in recent years highlighting mainly meteorological features of this event reconstructed on the basis of global reanalyses. Sodermann et al (2003) and Meneguzzo et al (2004), by using the NCEP/NCAR reanalyses to drive directly the limited area model RAMS, examined the sensitivity of the model precipitation in the Arno river basin with respect to model resolution, sea surface temperature, and initiation time. Bertò et al (2004, 2005) applied the backward trajectory method to the ERA-40 fields to study the areas of origin and the transport properties of water vapour in this and other cases of heavy precipitation in the Alps. De Zolt et al (2006) analysed the sensitivity of the precipitation field using the ERA-40 and NCEP/NCAR reanalyses as initial and boundary conditions for the limited area model BOLAM.

The purpose of this work is to revisit the main features of this extreme event, by exploiting the availability of global reanalysis and of up-to-date meteorological and hydrological prediction models. The aim here is to assess the possibility of a detailed “hindcast” (*a posteriori* forecast) of quantitative precipitation during a severe flood event and of the associated hydrological aspects like river flows, using “today tools with

yesterday data”. The system implemented for the present investigation simulates a forecast chain, starting from initial conditions derived from the ERA-40 reanalysis. Hereafter, the word “forecast” is used to stress that, for each model run, only data available at the initial condition time are used.

The event considered here was the most important in Italy in the last century, taking into account its spatial extension and overall intensity. Therefore, it represents an ideal test case to evaluate the capability of up to date, high-resolution meteorological and hydrological models to predict extreme floods. Such models are becoming more and more useful in the short-range forecasting (Gouweleeuw et al, 2004). Attention will be focused on the prediction of small-scale features of weather and flood hydrographs, rather than on the prediction of the synoptic, large-scale characteristics of the atmospheric evolution. In particular, emphasis will be put on the verification of predicted precipitation over the whole flooded areas and at the scale of hydrological basins.

The paper is organised as follows. The meteorological analysis of the event is outlined in Section 2. The model characteristics and experimental set-up are described in Section 3. In Section 4, the results of the meteorological and hydrological integrations are presented and discussed also in comparison with the aforementioned studies. Finally, the conclusions are drawn in Section 5.

## **2. Meteorological analysis**

### **2.1 Synoptic description**

The period preceding the event was characterised by the presence of an Atlantic blocking pattern west of the British Isles (Figure 1a), that started collapsing quickly between 1 and 2 November, when a mid tropospheric trough deepened on the eastern flank of the blocking ridge, extending from eastern Europe to Spain (Figure 1b). The trough was reinforced, between 3 and 4 November, by another fast-moving trough coming from the northern Atlantic (Figure 1c and d). At the surface, cyclogenesis started over Spain and moved over the western Mediterranean (Figure 1e). A simultaneous intensification of an anticyclone occurred over the Balkans (Figure 1e and f). The whole structure appears as a unique amplifying baroclinic wave with westward tilt with height, embedded in a strong large-scale meridional temperature gradient ranging from the Atlantic off of Morocco to the eastern Mediterranean, at latitudes between 30° and 40° N (not shown).

The lowest mean sea level pressure (mslp) over northern Italy at 12 UTC of 4 November was not very deep (about 994 hPa, see Figure 1f). Nonetheless, the west-to-east pressure gradient over Italy and the Adriatic Sea became very large around this time and was associated with exceptionally strong pre-frontal southerly winds. The dramatic intensification of the synoptic-scale zonal gradient of geopotential and mslp, visible in Figure 1d and f, respectively, was associated with the formation of a very strong, warm meridional flow to the east of the advancing cold front. This current can be identified with a Warm Conveyor Belt (WCB, Browning and Roberts, 1994) and also with an “atmospheric river” (Zhu and Newell, 1998; Ralph et al, 2004), due to the presence of a very large flux of moisture from northern Africa (Bertò et al, 2005).

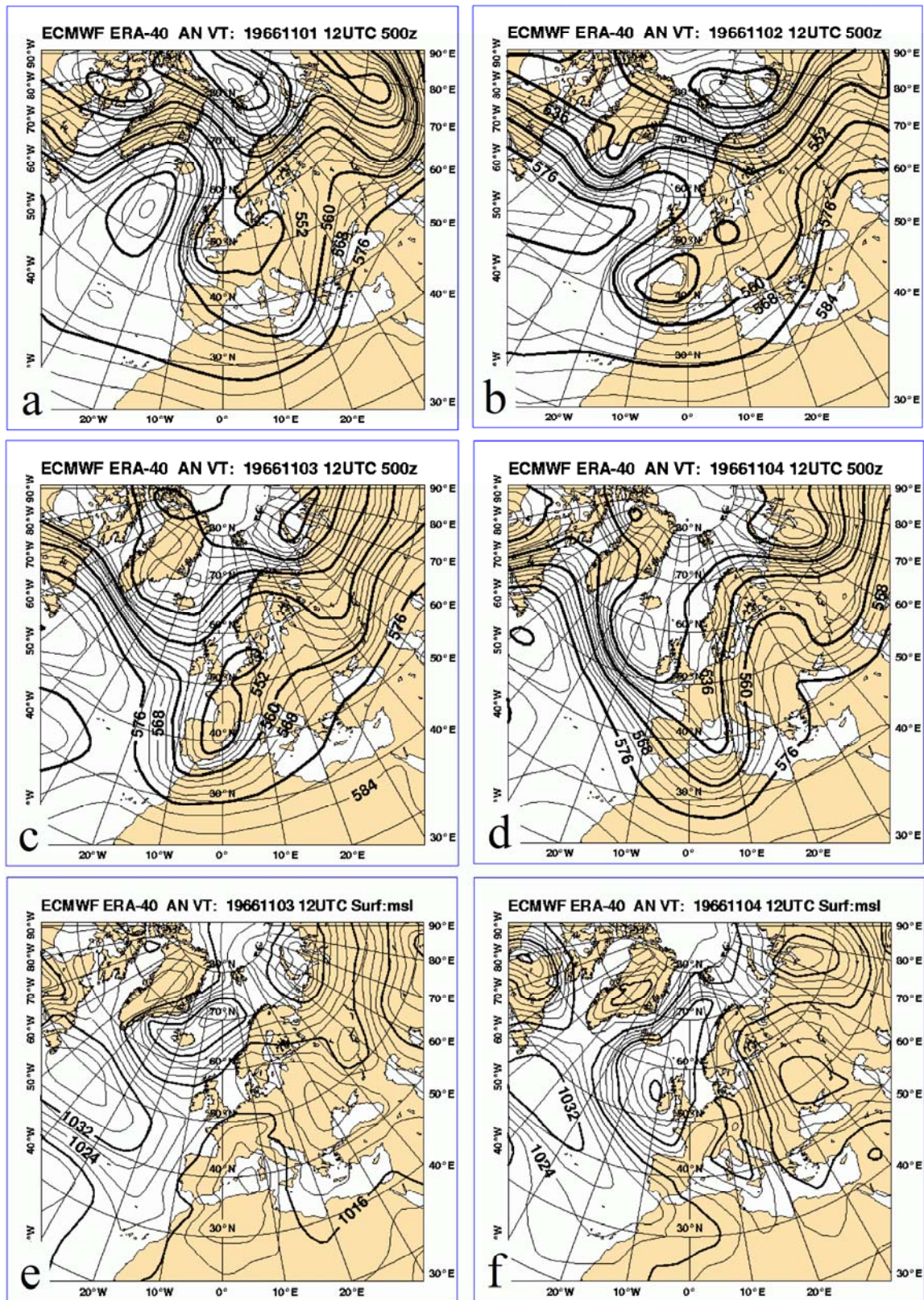


Figure 1 ERA-40 maps of geopotential height (a, b, c, d) at 500 hPa (contour interval: 40 m) and of mslp (e, f, contour interval: 4 hPa). a: 1 Nov. 1966, 12 UTC; b: 2 Nov. 1966, 12 UTC; c and e: 3 Nov. 1966, 12 UTC; d and f: 4 Nov. 1966, 12 UTC.

## 2.2 Mesoscale features

On the mesoscale, the evolution of the low level cyclone appeared to be characterised by multiple pressure minima at 00 UTC of 4 November (see Figure 2, showing a composite of surface hand-made analyses by Fea et al, 1968), moving northward and embedded in a meridionally elongated trough. A north-south oriented cold front was moving slowly north-eastward: the blue line denotes its position 12 hours later. The “warm front” drawn in Figure 2 over the Po Valley actually corresponds to a quasi-stationary boundary that separates the southerly flow from the cold air pool trapped south of the Alps, which is associated with an easterly barrier wind (Buzzi, 2005). Strong radar echoes, indicative of deep convection, were detected roughly at the same time along an almost north-south straight line slightly in advance of the cold front (green spots in Figure 2). Fea et al (1968) report that echo tops reached 11,000 m in the northern half of the convective line. Thunderstorm reports are visible on the weather map in the same figure where the northern portion of the convective line intersects the land.

In the first hours of 4 November, the easterly flow over the Po Valley changed into a southerly flow rising over the mountain slope, contributing to strong orographic precipitation. The rapid pressure decrease (see the pressure tendency analysis in Figure 2) reflects the cold air removal. The intense precipitation over the eastern Alps started in association with this regime transition between “blocked flow” at low levels and “flow over”. The rising flow over the southern flank of the Alps was nearly moist adiabatic. In this kind of situations, precipitation depends basically on the strength and humidity of the impinging flow, and is therefore more predictable than convective precipitation.

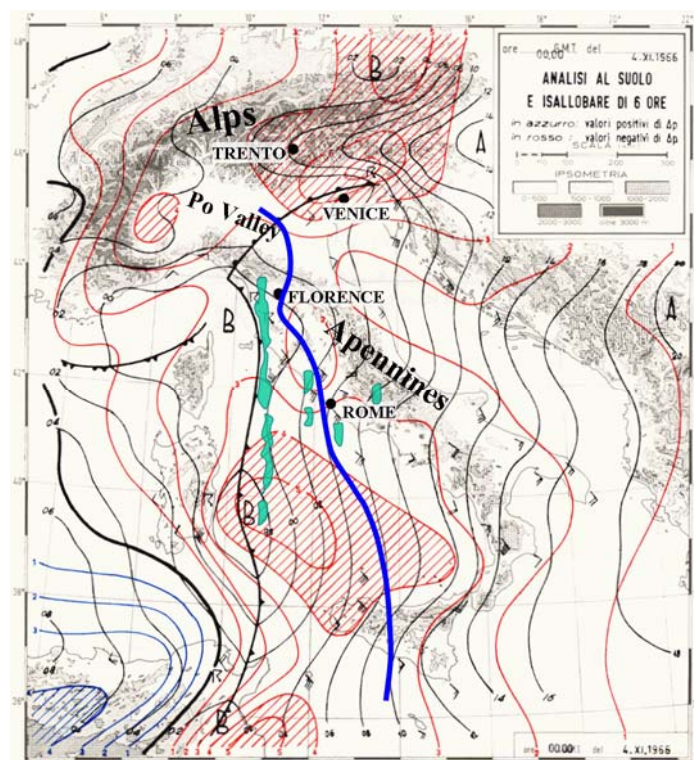


Figure 2 Weather map re-elaborated from handmade analyses published in Fea et al. (1968). The basic meteorological fields refer to 4 Nov. 1966, 00 UTC. Continuous black lines: mslp, (contour interval 2 hPa). Coloured thin lines: pressure tendency in 6 hours (blue: positive; red: negative; contour interval hPa/6h). Wind barbs in knots. Low pressure centres: B; high pressure: A. The green spots reproduce reflectivity maxima of the meteorological radar in Rome Fiumicino, at 00:40 UTC, same day. The thick blue line indicates the position of the cold front at 12 UTC of the same day

The change in wind regime is illustrated in Figure 3, which shows a time-height cross section of meteorological parameters deriving from the Udine radio sounding station (see location in Figure 4) redrawn from Fea et al (1968). The period ending at 00 UTC of 4 November was characterised by a continuous warming, more pronounced at mid tropospheric levels (left panel of Figure 3). The highest (in time) temperatures were observed at 00 UTC in a layer between 3 and 4 km, when the freezing level raised up to about 3700 m, starting from a height of about 1500 m on 2 November. Near the surface, the warmest spell was observed around 12 UTC of 4 November, with temperature rising up to 16-17 °C all along the coast of the northern Adriatic Sea. Saturated or nearly saturated conditions were encountered below 3 km in the entire two-day period preceding the arrival of the cold front. The right panel of Figure 3 shows the profiles of wind and specific humidity. The clockwise rotation and intensification with height of the wind vector in the first km above the surface, at 00 UTC of 4 November, was due to the orographic blocking mentioned above. By 12 UTC of 4 November the south-south-easterly wind exhibited a maximum speed of 70 knots (35 m/s) at a height between 1500 and 2000 m. At the surface, the maximum intensity of the Sirocco (south-easterly) wind recorded in Venice was 18 m/s at 15 UTC. Consistently with these observations, the ERA-40 reanalysis shows a wind speed maximum of 32 m/s in the layer between 950 and 850 hPa, with 10 m wind maximum of about 20 m/s over the northern Adriatic Sea.

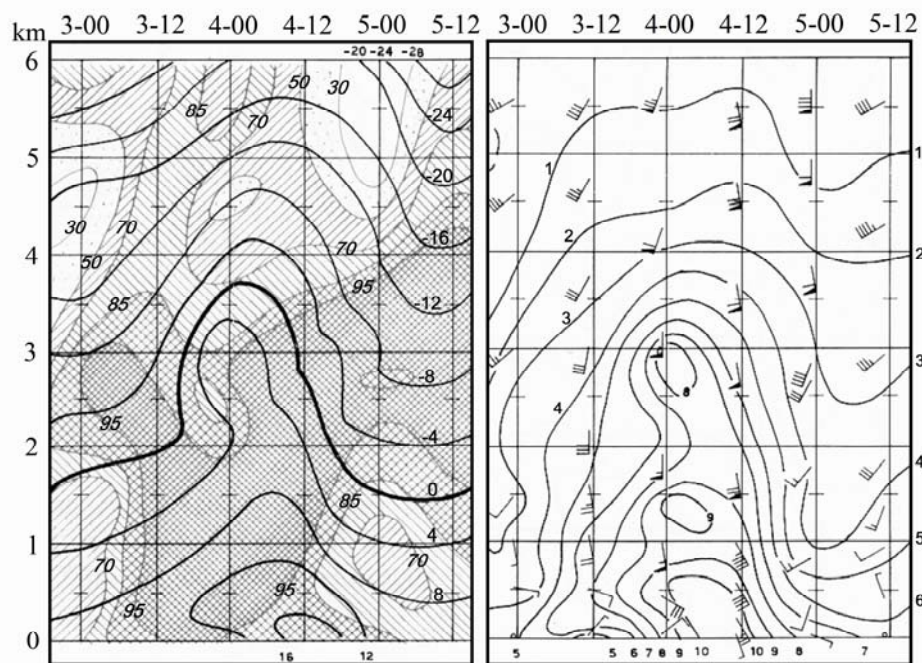


Figure 3 Time (in abscissa, day - UTC hours at the top) and height (in ordinate, from the surface to 6 km) section, based on the Udine (16044) radio-sounding data, every 12 hours, for the period 3 to 5 Nov. 1966, re-elaborated from Fea et al (1968). In the left panel, temperature (deg. Celsius, thick lines) and relative humidity (hatched) are indicated. In the right panel, wind (with conventional symbols, in knots) and specific humidity contours (gr/kg).

In summary, the south-easterly wind over the Adriatic, that forced the sea level surge (198 cm in Venice, the highest ever recorded) and the orographic precipitation on the southern flank of the Alps can be considered as the most relevant atmospheric features characterising this extreme event. The pre-frontal flow, which assumed the character of a strong WCB and of an atmospheric river, was very moist, unstable over central

Italy and nearly neutral upstream and over the Alps. It accounted for a very large meridional transport of water vapour. By considering the contribution of the low level southerly jet in a layer 3 km deep and 200 wide, and by using the specific humidity and wind values reported in Figure 3 at 12 UTC of 4 November, a flux of water of about  $1.2 \times 10^8$  kg/s impinging over the eastern Alps can be estimated. This value is comparable with that of  $1.5 \times 10^8$  kg/s quoted, for example, by Ralph et al (2004) as typical of atmospheric rivers over the eastern, North Pacific Ocean. For the Alps, during the Mesoscale Alpine Programme (MAP), Smith et al (2003) have estimated an “efficiency” of orographic precipitation of 35%, defined as the ratio between total precipitation rate and incoming vapour flux. This value, though very sensitive to both dynamical and microphysical aspects, allows an estimate of the amount of orographic precipitation that can be produced when an atmospheric river intersects a mountain chain.

### 2.3 Accumulated precipitation

The 2-day accumulated precipitation measured at rain gauge stations is presented in Figure 4, superimposed on the precipitation field predicted by one of the high-resolution runs (see the following sections 3 and 4). The analysis is based on a network of 1296 stations, sufficiently dense to resolve mesoscale features of the order of a few tens of km. Original observations were published on the 1966 annual report of the Italian Servizio Idrografico e Mareografico Nazionale (Ministero dei Lavori Pubblici, 1970). The accumulation period of observations spans the time range from 08 UTC of 3 November to 08 UTC of 5 November.

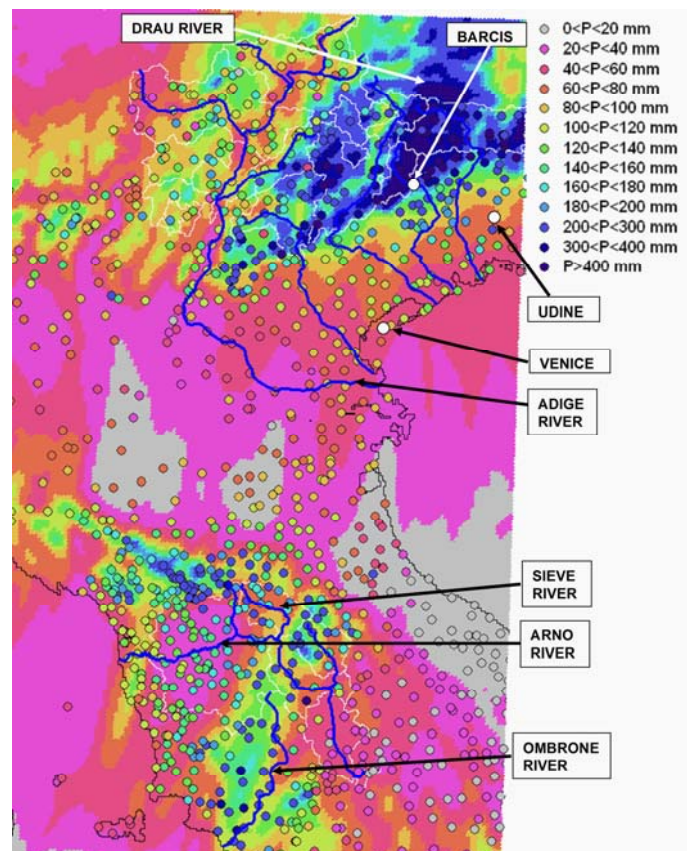


Figure 4 Observed 48 h accumulated rainfall (circles) in the period ending 5 Nov. 1966, 08 UTC, superimposed over the precipitation field produced by MOLOCH for Exp3CONV (see text). The blue lines represent the major rivers described in the paper; white lines the major watershed divides.

Over the eastern Alps an elongated maximum, with several values exceeding 500 mm, extends over the pre-alpine slope, with a well-defined minimum over the Adige valley. The highest value (751 mm in 48 hours) was recorded in the station of Barcis. Large precipitation amounts, in the range 200-400 mm, were also observed further north, at the alpine divide. Severe flooding affected all the main rivers from the Adige catchment to the east, including the Drau river north of the main crest. At most of the streamflow stations and artificial reservoirs, river level records and discharges were the highest ever recorded since the end of the 19<sup>th</sup> century. Up to 2 m<sup>3</sup>/s/km<sup>2</sup> of runoff peak were recorded in basins as large as 2000 km<sup>2</sup>, and more than 2 m<sup>3</sup>/s/km<sup>2</sup> for basins of 400 km<sup>2</sup> in size. Precipitation in the alpine region was due mainly to the orographic uplift, in stable or neutral (moist) conditions.

The other main flooding area, corresponding to the Arno and Ombrone rivers, is characterised by a well-defined precipitation band, with values in excess of 300 mm in two days, which extends from the Tyrrhenian coast towards north-east, where the springs of the Arno river are located. Up to 1.2 m<sup>3</sup>/s/km<sup>2</sup> of runoff peak were recorded in the Ombrone river at Sasso d'Ombrone, gauging an area of 2657 km<sup>2</sup>, and the specific flood peak of the Arno river at Subbiano (see Figure 8), gauging an area of 738 km<sup>2</sup> in size, was about 3 m<sup>3</sup>/s/km<sup>2</sup>. As anticipated in the previous sub-section, there is evidence both from SYNOP and radar observations (see Figure 2), that deep convection contributed to this precipitation maximum. A secondary maximum is observed upstream and above the northern Apennine divide, partly in the Sieve river basin, tributary of the Arno river. This maximum is clearly due to an orographic forcing, although it is not possible to separate the contribution of convection to the total precipitation fallen in this area. Floods, though less severe than in Tuscany, also affected rivers flowing north of the Apennines.

### 3. Models and methodology

#### 3.1 Meteorological models

The initial conditions for the European Centre Medium-range Weather Forecasts (ECMWF) global prediction model, used in the present study, were taken from the T<sub>L</sub>159L60 (where 159 is the horizontal spectral truncation and 60 the number of vertical levels) ERA-40 reanalysis, having the horizontal resolution corresponding to roughly 130 km along a meridian. It should be recalled that in 1966 there were no satellite and very few aircraft data, while the number of conventional data was within a factor of two from the number available today (Simmons and Gibson, 2000; Uppala, 2001; Uppala et al, 2005). This has clearly an impact on the quality of ERA-40 analysis. Considering, for example, one-day forecasts for the 500 hPa geopotential height over the northern hemisphere, Uppala et al (2005) report that the average error of forecasts started between 1958-1960 is about 40% larger than the error of forecasts started between 1989 and 1991.

A series of forecasts of the ECMWF global spectral model with resolution T<sub>L</sub>511L60 were performed starting at different initial condition times. This model version (cycle 23r4) was used operationally at ECMWF between 12 June 2001 and 22 January 2002 (see Simmons, 2001; Uppala et al, 2006). In cascade, high resolution, limited area meteorological forecasts have been made using the one-way, multiple nesting technique, having as initial and boundary conditions the fields derived from the ECMWF forecasts. A large downscaling factor (about 60 in the present case) is needed, since the hydrological applications to small size basins, typical of the area under investigation, require a few km resolution precipitation fields. With this approach it is tested the capability of a purely dynamical downscaling, in the assumption that small scales

can be consistently reconstructed from the large scale atmospheric dynamical features, and by prescribing the appropriate topographic forcing.

The limited-area models used in this study are BOLAM and MOLOCH, both developed at ISAC-CNR. BOLAM is a meteorological model based on the primitive equations in hydrostatic approximation. It uses sigma-coordinates and wind components, potential temperature, specific humidity, surface pressure, and concentration of five hydrometeor classes as dependent variables, distributed on a non-uniformly spaced Lorenz grid. The horizontal discretization uses geographical coordinates, with latitudinal rotation on the Arakawa C-grid. The model implements a “Weighted Average Flux” (WAF, Billet and Toro, 1997) scheme for the three-dimensional advection. The lateral boundary conditions are imposed using a relaxation scheme that minimises wave energy reflection. A detailed description of the dynamics and numerical schemes can be found in Buzzi and Foschini (2000). The water cycle for stratiform precipitation is described by means of a simplified approach similar to that proposed by Schultz (1995). Deep convection is parameterised using the Kain-Fritsch convective scheme (Kain and Fritsch, 1990; Kain, 2004). The surface and boundary layer parameterisation is based on the *E-I* approximation, in which turbulent kinetic energy is predicted explicitly. Surface processes consist in the water and energy balance in a three-layer ground model. The atmospheric radiation is computed with a combined application of the Geleyn (Ritter and Geleyn, 1992) and ECMWF scheme (Morcrette, 1991; Mlawer et al, 1998). The initial and boundary variables are obtained by interpolating the atmospheric, surface, and ground variables from the ECMWF model forecasts to the higher resolution BOLAM grid.

MOLOCH is a non-hydrostatic, convection-resolving model. It integrates the fully compressible set of equations with prognostic variables (pressure, temperature, specific humidity, horizontal and vertical velocity components, and five water species) represented on the lat-long rotated, Arakawa C-grid. Terrain following coordinates, relaxing smoothly to horizontal surfaces away from the earth surface, are employed. Model dynamics are integrated in time with an implicit scheme for the vertical propagation of sound waves, while explicit, time-split schemes are implemented for the remaining terms. Three-dimensional advection is computed using the eulerian WAF scheme. Horizontal fourth order diffusion and divergence damping are included to prevent energy accumulation on the shorter space scales. The physical scheme consists of radiation (as for BOLAM), sub-grid turbulence, microphysics, and soil water and energy balance. The turbulence scheme is based on an *E-I* closure, where the turbulent kinetic energy equation (including advection) is evaluated. Surface turbulent fluxes of momentum, specific humidity, and temperature are computed by the classical Monin-Obukhov theory with Businger / Holtslag functions in the unstable / stable case. The mixing length is computed from turbulent kinetic energy (Deardorff, 1980) in the stable atmosphere and from Bougeault and Lacarrere (1989), modified by Zampieri (2004), in the unstable environment. The microphysical scheme is based on the parameterisation proposed by Drofa and Malguzzi (2004). The physical processes determining the time tendency of specific humidity, cloud water/ice and precipitating water/ice are divided into “fast” and “slow” ones. Fast processes involve transformations between specific humidity and cloud quantities and are computed every advection time step. Temperature is updated by imposing exact entropy conservation at constant pressure. Fall of precipitation is computed with the stable and dispersive backward-upstream scheme, with fall velocities depending on concentration. The soil scheme used here is similar to the one of BOLAM. MOLOCH is nested into the BOLAM runs performed at coarser resolution.

The period of interest for the meteorological and hydrological forecasting has been identified in the 48 h time span from 08 of 3 November to 08 of 5 November 1966. This covers almost the entire precipitation period and corresponds to the rain-gauge accumulation interval of 2 days (ending each day at 8 UTC). This constraint has determined the forecast interval for the highest resolution meteorological model. The total forecast time, considering the initial time of the global ECMWF model, has been varied in the range between 54 and 78 hours. This allows the assessment of forecast quality as a function of the forecast duration.

Table I shows the initial condition times for each model run, the model grid spacing being indicated in the first row. There is roughly a downscaling factor of 3 between consecutive nesting steps. The domain extension in lat-lon degrees is also indicated. The MOLOCH domain is elongated in latitude to embrace the two main precipitation areas. Boundary condition updating is performed every 3 hours for BOLAM\_18 (18 km grid spacing), every 1.5 hours for BOLAM\_6, and every hour for MOLOCH.

*Table 1 Initial conditions for the meteorological forecast chain. Horizontal grid spacing, number of vertical levels, and the size of the integration domain are reported for each meteorological model.*

Experiments	ECMWF T511, L60, global	BOLAM_18 18 km, L38, 27x27°	BOLAM_6 6 km, L44, 11x11°	MOLOCH 2.2 km, L50, 4x6.6°
Exp1CONV	2 Nov. 00 UTC	2 Nov. 00 UTC	3 Nov. 06 UTC, conv.	3 Nov. 07 UTC
Exp1NOCONV	-	-	3 Nov. 06 UTC, no conv.	3 Nov. 07 UTC
Exp2CONV	2 Nov. 12 UTC	2 Nov. 12 UTC	3 Nov. 06 UTC, conv.	3 Nov. 07 UTC
Exp2NOCONV	-	-	3 Nov. 06 UTC, no conv.	3 Nov. 07 UTC
Exp3CONV	3 Nov. 00 UTC	3 Nov. 00 UTC	3 Nov. 06 UTC, conv.	3 Nov. 07 UTC
Exp3NOCONV	-	-	3 Nov. 06 UTC, no conv.	3 Nov. 07 UTC

At 6 km, BOLAM tends to produce explicit convective precipitation with unrealistic spatial scales. Existing parameterisation schemes are not meant to work properly at such a high resolution, due to the fact that there is no clear scale separation between sub-grid and explicitly represented convection (Kain, 2004; Warner and Hsu, 2000). The inner MOLOCH model does not have this problem, since it is capable of representing convection explicitly. When the 6 km model parameterises convection, the inflow atmospheric profiles tend to be more stable, therefore decreasing the potential for development of convection by the non-hydrostatic inner model. In the opposite case, i.e. without convective parameterisation in the outer domain, errors due to the misrepresentation of convective scales can adversely affect the inner domain simulation through boundary condition influence. Since there is no general remedy to this problem, except enlarging the inner domain as much as possible, it was decided to perform, for each experiment, two different runs of BOLAM\_6, with and without activation of the parameterisation of convection (named, respectively, ‘CONV’ and ‘NOCONV’ in Table 1). Therefore, six 2.2 km forecasts and associated input precipitation fields are available for the hydrological model.

### 3.2 Hydrological model

The hydrological model employed here (DIMOSOP) is a conceptual distributed model, previously used to simulate past flood events (Bacchi et al., 2002; Bacchi and Ranzi, 2003) and to produce real-time forecasts in the Toce river basin (Piedmont, north-western Italy) during the MAP Special Observing Period (Ranzi et al., 2003; Grossi and Kouwen, 2004). The conceptual scheme adopted to estimate the rainfall partitioning into interception, runoff and infiltration is the Curve Number Method, widely investigated by the U.S. Soil

Conservation Service (see U.S.D.A., 1986), and successfully tested in several Italian basins. It assumes that the storm runoff volume is proportional, at each computational time step, to the rainfall volume exceeding a threshold, through the ratio between the accumulated infiltration and the soil water storage capacity. The threshold represents initial water losses mainly due to depression storage and interception. The flood routing process is represented through a dynamic Muskingum-Cunge scheme, solving the linear parabolic convection-diffusion equation. Different hydraulic parameters are used to discriminate overland and channel flow, as described in Ranzi et al. (2002).

For the Arno case, the topography was obtained from a 250x250m Digital Elevation Model (DEM). This DEM was used to automatically extract the river network (Figure 8) that determines the flood routing. The parameters describing the river channel geometry were assumed on the basis of surveys on the investigated basins, as reported by Orlandini and Rosso (1998). The time lag in some sub basins of the Arno river was derived from the application of the pioneering mathematical model of Natale and Todini (1977). The soil hydrological properties and the storage capacity parameter were derived, using the standard procedures suggested by U.S.D.A., from the permeability and land-use maps provided by the Arno Water Authority. The permeability values were quite in agreement with other maps of soil hydraulic properties produced for some selected areas in the Arno basin (see Becchi et al, 1995).

## 4. Results and discussion

### 4.1 Meteorological forecasts

In this section the focus is put on the validation of the precipitation fields. The ECMWF precipitation (Figure 5) and the corresponding MOLOCH precipitation (Figure 6), accumulated over the period of interest, are presented for all the experiments listed in Table I. MOLOCH precipitation of Exp3CONV, with convective parameterisation activated in the BOLAM\_6 run, is also plotted in Figure 4 using the same palette as observed data, in order to facilitate the comparison between predictions and observations.

The ECMWF model is able to predict the two main precipitation spots over the Alps and near the Tyrrhenian side of Central Italy in all the forecasts. With reducing forecast validity, the position of precipitation centres tends to be more correctly located but with strong underestimation of maxima, especially over the Alpine region. The forecast starting at 00 UTC of 2 November (Figure 5a) shows a very broad precipitation pattern over the Alps, with a maximum of about 255 mm and a secondary maximum of 190 mm over the north-western part of Tuscany. However, the main precipitation band over central-southern Tuscany is totally missed. The highest value over the eastern Alps, in excess of 300 mm, is predicted starting at 2 November, 12 UTC (Figure 5b), while the maximum over Tuscany is shifted towards the correct position but with weak intensity. The last forecast experiment (Exp. 3, Figure 5c) predicts more accurately the position of the Tuscany maximum, though the precipitation amount is still underestimated. The same holds for the Alpine maximum, which is more precisely located with respect to the earlier starting forecasts.

The corresponding high-resolution precipitation fields (Figure 6), although reflecting the much more detailed scales of the orography and of the convective dynamics, show overall similar features in terms of changes of the initial conditions. The precipitation amount and spatial distribution over the Alps are definitely more realistic, although the absolute maximum varies between an underestimation of 673 mm (Exp3CONV) and an overestimation of 1050 mm (Exp2, both CONV and NOCONV), as a function of the initial condition time. Over Tuscany, there is still an underestimation of the total precipitation but, at variance with ECMWF

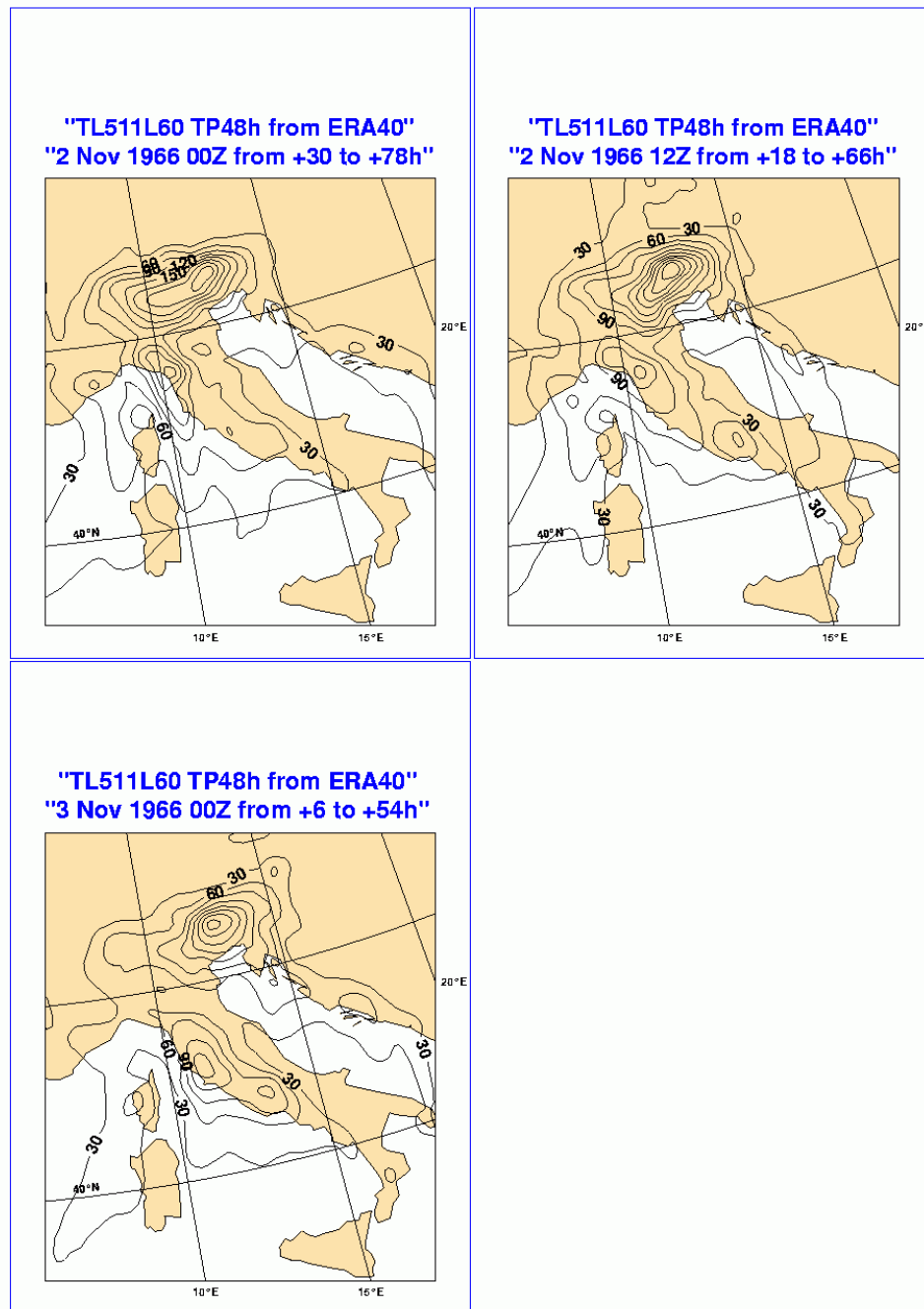


Figure 5 48 h accumulated precipitation, in the period ending 5 Nov. 1966, 06 UTC, for the ECMWF forecasts (see text) starting: a: 2 Nov. 00 UTC; b: 2 Nov. 12 UTC; c: 3 Nov. 00. Contour interval: 30 mm. Precipitation maxima in the two main areas are reported.

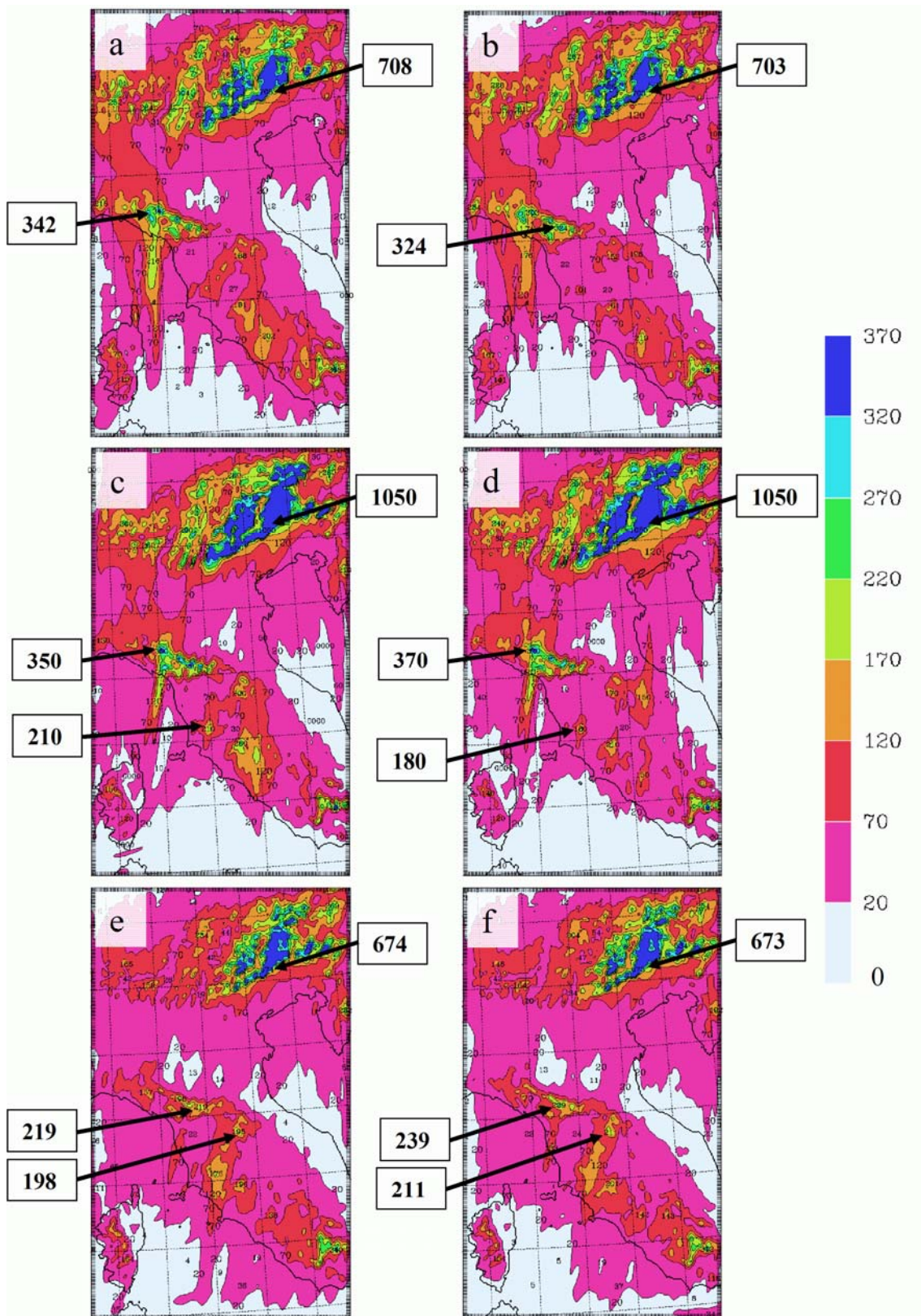


Figure 6 47 h accumulated precipitation, in the period ending 5 Nov. 1966, 06 UTC, for the six MOLOCH forecasts nested in the BOLAM forecasts reported in Table I: a: Exp1NOCONV; b: Exp1CONV; c: Exp2NOCONV; d: Exp2CONV; e: Exp3NOCONV; f: Exp3CONV. Contour interval: 30 mm. The main precipitation maxima are indicated.

forecasts, strong precipitation upstream of the Apennines, in the catchment area of the Arno river, is now forecasted. In particular, in Exp. 3 (Figure 6 e-f) the two separate maxima over Tuscany appear in the correct position. Over the Po Valley, north of the Apennines, observations show an area of relatively weak precipitation around 50 mm. This indicates that no important convective precipitating system occurred over this region. The high-resolution model catches this feature, though the precipitation amounts in the lee (north) of the Apennines are generally underestimated. In summary, the high-resolution meteorological fields produced by Exp3 (CONV and NOCONV) give the best results. Inspection at Figure 4 reveals a good agreement between observed and predicted precipitation in the north-eastern Alpine region, in terms of both 1 maximum locations and precipitation amounts. Over Tuscany, the main rainfall band with predicted precipitation amounts over 200 mm is well located, but underestimated when compared to the observed values, which are in excess of 300 mm.

Similar conclusions can be drawn by inspection of Figure 7, which shows a scatter diagram of predicted versus observed accumulated precipitation, integrated over several river basins and relative sub-basins located in Tuscany and northern Italy (see also next subsection). The points enclosed by circles are relative to Arno sub-basins and major tributaries, whose geographical location is shown in Figure 8. It can be seen that over the alpine river basins (their watershed divides are marked by white lines in Figure 4) there is no systematic error, while precipitation over the Arno river is, on average, under-predicted. It can be noticed, in particular, the underestimation over the Sieve river basin.

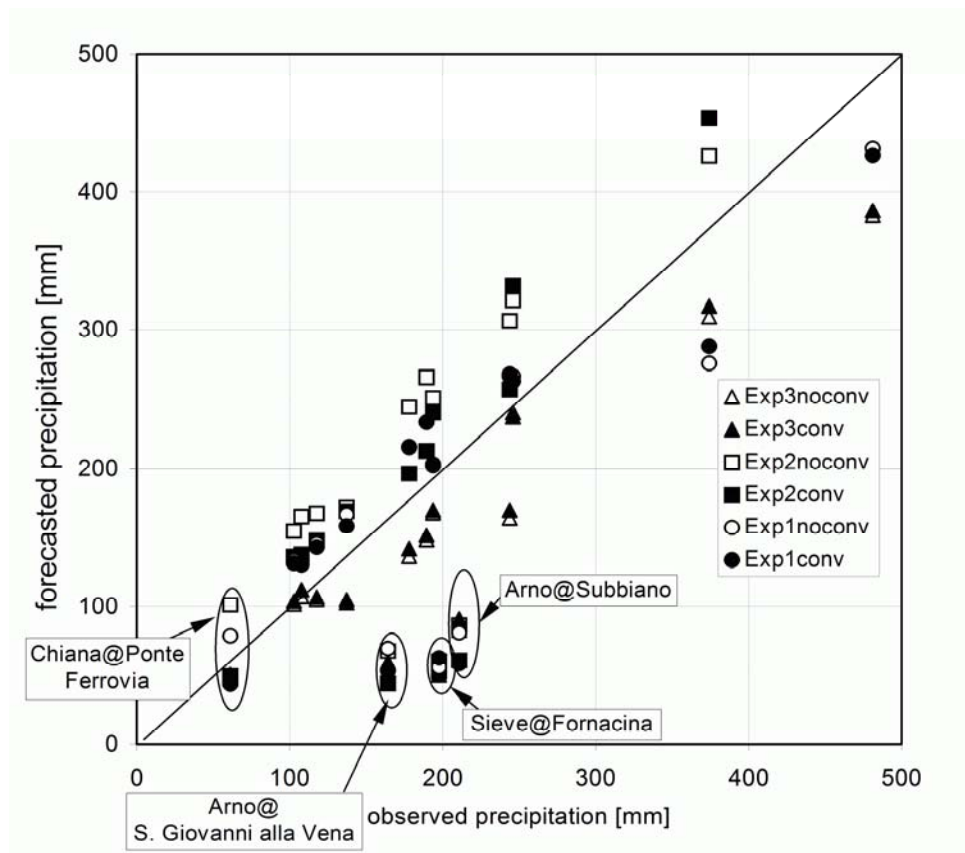


Figure 7 Observed and forecasted total precipitation (48 hours) in the Arno river basins and in some alpine basins delineated in Figure 4.

Observed (and predicted) precipitation timing is closely associated with the movement of the frontal line from west to east and to the corresponding low level southerly jet (WCB), as discussed in section 2. The forecast of the frontal propagation turns out to be sensitive to the time of the initial condition. In general, the lower resolution models tend to overestimate the frontal speed (not shown). This, in turn, implies a reduction of precipitation amounts predicted over central Italy by the higher resolution models.

The aforementioned publications by Sodermann et al (2003) and Meneguzzo et al (2004) allow only a qualitative inter-comparison between the precipitation fields obtained with the high resolutions models over Tuscany, due to the different set-up conditions and initialisation times, and to the use of NCEP/NCAR reanalyses in place of global forecasts. Broadly speaking, the precipitation distributions and amounts simulated in the above-mentioned papers are comparable with those of MOLOCH Exp.3. De Zolt et al (2006), by contrasting the precipitation simulations based on the different (ECMWF and NCEP/NCAR) analyses, show that differences are associated with visible discrepancies between the two data sets. In particular, the simulation based on NCEP/NCAR reanalysis seems more accurate in reproducing the main precipitation band over the Ombrone river.

Concerning the MOLOCH predictions with and without convective parameterisation activated in the BOLAM\_6 runs, the main differences are noticed, as expected, in the areas where convective activity develops, namely over the Tyrrhenian Sea and central Italy. These areas are located just downstream, with respect to the mean tropospheric flow, the boundaries where the properties of the inflow depend on the activation of convective parameterisation in the BOLAM\_6 model. In such areas, precipitation at 2.2 km is, on average, slightly larger in the NOCONV experiments. Due to the presence of explicit convective cells in the MOLOCH runs, the rainfall patterns are anisotropic, being elongated in the direction of cell propagation. In the CONV experiments, the explicit convective cells in MOLOCH initiate later, i.e. downstream and farther away from the south-western boundaries, due to the more stable inflow profiles. This effect, however, does not extend north of the Apennines. Over the alpine region the precipitation pattern and intensity is hardly affected by the switch of parameterised convection in the driving model, suggesting that orographic uplift is the main mechanism for precipitation formation in that area.

## 4.2 Hydrological forecasts

The precipitation fields produced by MOLOCH were used to force the DIMOSOP hydrological model in order to reproduce the flood hydrograph at the sections of the Arno river and of its main tributaries shown in Figure 8. Flood predictions were done also for most of the sub-basins, outlined in Figure 4, in the Alpine area. Only results obtained with Exp3 (CONV or NOCONV) are presented here since, as shown in the previous subsection, this experiment gives the best prediction from the meteorological point of view.

It is notable that MOLOCH at 2.2 km computes the precipitation field at a spatial resolution much higher than the density of rain gauges. In fact, while most of the rain gauges working at the time of the event provided daily amounts, only a subset recorded the rainfall time series continuously. In order to check separately the validity of the hydrological model, a "control" run was first performed for each basin, using the hourly precipitation time series recorded by the gauges available within the basin itself. Areal precipitation was computed by implementing a Thiessen interpolation procedure; the same procedure, in practice a nearest-neighbour interpolation, was applied to distribute the forecasted precipitation fields. No calibration of the hydrological and hydraulic parameters was done after the initial model set-up.

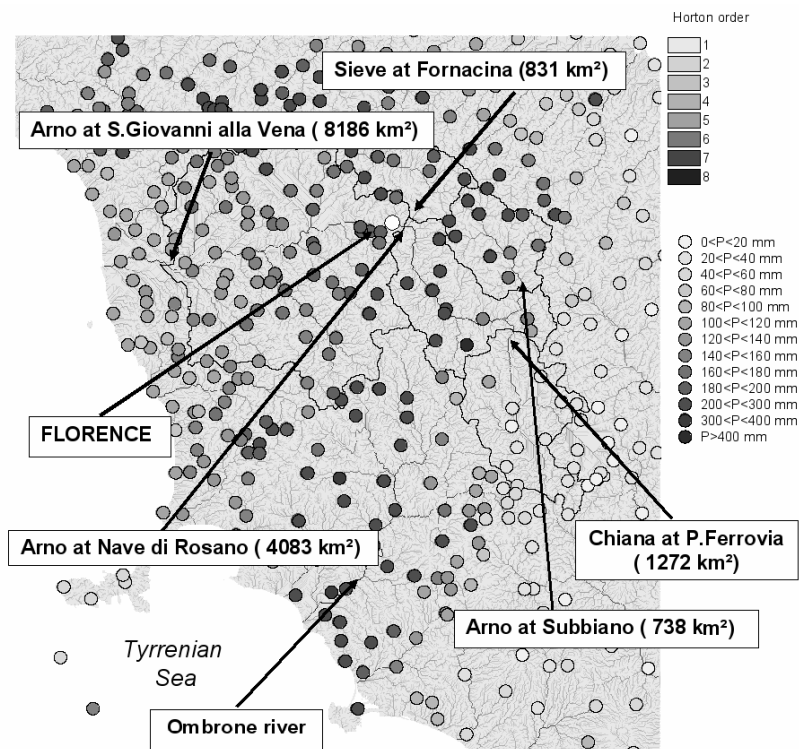


Figure 8 The river network derived from the 250 m Arno basin DEM. Horton orders of river channels are represented. Watershed divides of major sub-basins are reported.

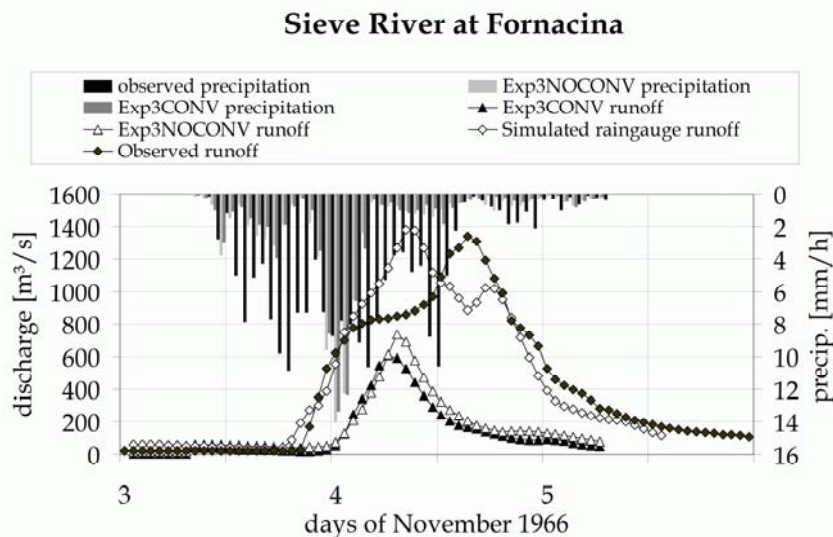


Figure 9 Observed and forecasted flood hydrograph for the Sieve river at the section of Fornacina. Forecasted precipitation from Exp3.

For the Arno watershed, the complete observed hydrograph was actually available for the section of the Arno river at S.Giovanni alla Vena and for the section of the Sieve river at Fornacina. For the other river sections, only the peak discharge and part of the flood hydrographs (generally the rising limb) were recorded before the flood damaged the instrumentation. Results are shown here for the Fornacina closure section only (see in Figure 9 the complete hydrograph). The control run shown in Figure 9 is satisfactory in reproducing the

ascending and descending part of the hydrograph, as well as the total runoff volume and peak discharge values, but does not reproduce the plateau in the observed hydrograph. This is probably due to the fact that the few recording rain gauges (only 6 gauges reported hourly precipitation over the Sieve basin) were not completely representative of the rainfall area distribution. The “upside-down hyetograph” shows rain rate time series averaged over the basin area. As shown in Figure 7 for the river Sieve at Fornacina, the differences between the CONV and NOCONV experiments are very small. In both cases, the timing of maximum precipitation intensity is good, but the peak duration is too short. Concerning predicted hydrographs, the shape of their evolution is quite similar to the control case, although the under-estimation of precipitation intensity, before and after the maximum, induces an under-estimation of runoff volumes and discharge peaks at the closure section.

The discrepancy between predictions and observations is lower for the wider area of the Arno river at S. Giovanni alla Vena (not shown), which is less sensitive to the errors in the spatial location of precipitation maxima. In fact, the geomorphology and soil characteristics of the Arno watershed suggest that the main tributaries to the flood in Florence came from the Sieve river basin at Fornacina (837 km<sup>2</sup>) and the upper Arno river basin closed at the section of Subbiano (738 km<sup>2</sup>). In the precipitation field of both the Exp3CONV and Exp3NOCONV experiments, the precipitation maximum, which occurred in part in the Sieve area, is shifted in the north-east direction. Therefore, the Sieve discharge underestimation is compensated by an over-estimation in the upper Arno basin.

Figure 10 reports a scatter plot showing control and forecasted versus observed peak flows over several river basins located in Tuscany and in the Alps, obtained from the Exp3CONV. This diagram shows that the peak flows are well reproduced in the control runs in both areas, while the forecasted peaks are well reproduced in the alpine basins but under-estimated in Tuscany, where the precipitation was mainly of convective type. In Figure 10, only the monitored sections upstream of Florence are reported, since the discharge observed at S. Giovanni alla Vena was strongly affected by breaches in the river levees and by the flooding of the area around and, especially, downstream the city of Florence. Exp3NOCONV (not shown) gives similar results.

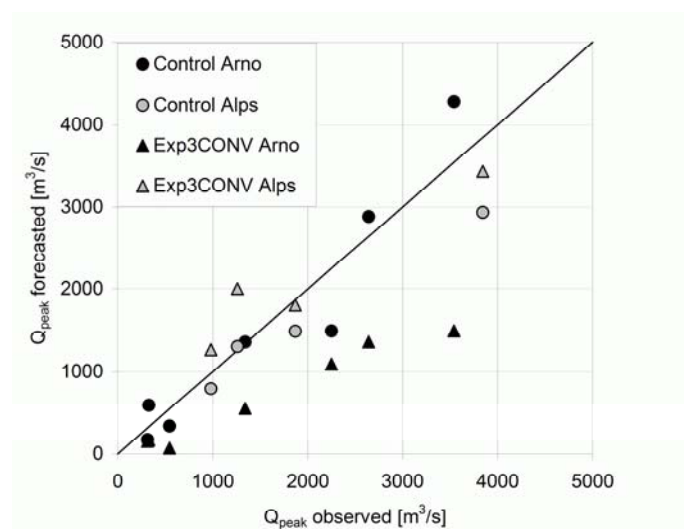


Figure 10 Scatter diagram of control/forecasted versus observed flow peaks for the Arno river and alpine basins. Different points correspond to different sub-basins or different closure sections. Forecasted precipitation from Exp3CONV.

Figure 11 shows the results of the hydrological control run and of the flood forecast in the small (392 km<sup>2</sup> in size) Cellina river basin at Barcis, in the eastern Alps, in the area where the maximum precipitation was measured. In this case, the control and forecasted flood hydrographs for the Exp3CONV experiment reproduce well the observations, both in terms of timing and discharge peak, while the total volume is slightly over-predicted. This hydrograph is representative of other results obtained for the Alpine area (see also Ranzi et al., 2004). Also for this case, Exp3NOCONV (not shown) gives similar results.

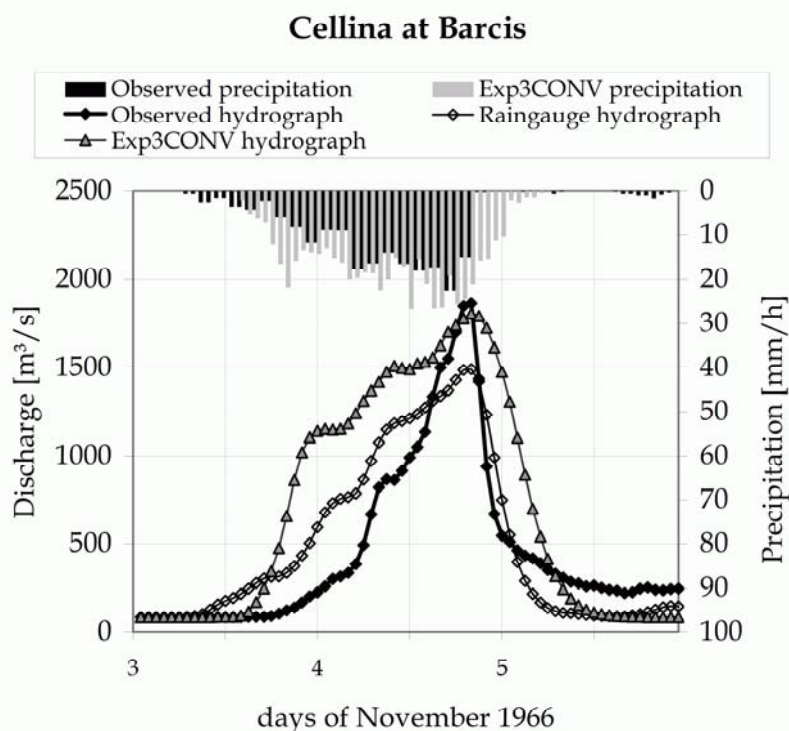


Figure 11 Observed and forecasted flood hydrograph for the Cellina river at the section of Barcis. Forecasted precipitation from Exp3CONV.

## 5. Conclusions

A meteo-hydrological forecasting chain was set-up to simulate the catastrophic flood that caused severe damages and loss of lives in several areas of Italy in early November 1966. This experiment was performed by nesting the non-hydrostatic MOLOCH model into the hydrostatic BOLAM, limited area meteorological model, in turn driven by the ECMWF global forecasts initialised with the ERA-40 reanalysis. With the resolution of 2.2 km of the inner MOLOCH model, small-scale spatial and temporal details of the meteorological fields relevant for the flood generation can be simulated. The DIMOSOP conceptual distributed hydrological model was employed to forecast hydrographs and discharge peaks, starting from the predicted high-resolution precipitation.

The quality of the meteorological forecast chain depends not only from the model characteristics, but also from the accuracy of the ERA40 reanalysis. In the period considered, the reanalysis quality is negatively affected by the absence of satellite data, which nowadays represent a basic source of information especially over oceanic regions. The data coverage dishomogeneity, when moving from the Atlantic ocean to continental Europe, can partly explain the degradation of the forecasts with increasing validity time,

considering that the large-scale disturbance responsible for this event was generated over the Atlantic. Only the forecast starting at 00 UTC of 3 November provided useful precipitation fields over the Tuscany area, where precipitation was mainly of convective type. Nevertheless, good forecasts of the exceptionally intense orographic precipitation over the eastern alpine region could be obtained with more than 48 hours in advance, as shows by Figure 6.

The high-resolution non-hydrostatic simulations were nested into intermediate-resolution hydrostatic runs performed with and without convective parameterisation. The experiments described in section 4 showed that, although the BOLAM runs without parameterisation of convection presented some important underestimation of precipitation amounts in the convective areas over central Italy, the impact on the MOLOCH results remained small, as indicated for example by the scatter diagram of Figure 7, and by the hydrographs of Figure 9. It would be erroneous, however, to draw general conclusions from inspection of a single case.

The 48 hours accumulated observed precipitation, averaged over several sub-basins in the north-eastern Alps and in the area of the Arno river, was compared with the corresponding predicted fields. The ground truth verification shows a general agreement, in the alpine area, of the forecasted fields initialised from 48 to 24 hours before the onset of the precipitation event. Concerning the Tuscany area, the timing of the forecasted precipitation is accurate, but the total amount is well reproduced only for the northern and southern part of the Arno basin, and is under-estimated in the other major upstream tributaries and downstream over areas close to the basin outlet, measuring about 8,000 km<sup>2</sup> in size.

Regarding the estimate of the forecast usefulness in terms of flood warnings, it can be concluded that, with the meteo-hydrological model chain here implemented, and with the meteorological observations available in 1966, an effective flood warning 24 to 48 hours in advance of the flood peak, that occurred in the afternoon of 4 November, could have been issued for the alpine region. However, for the Tuscany area, including the Arno river basin, realistic amounts of precipitation could only be predicted in advance of about 24 hours, and even that with important local under-estimations. Therefore, for the latter area, a timely warning based purely on model tools could only have been issued from 12 to 18 hours in advance of the precipitation peak, and about 24 hours before the flood peak.

### Acknowledgements

The Arno River Water Authority is acknowledged for the permeability and land-use maps provided. The Pisa branch of the hydrographic service is thanked for having provided some hydrometric data.

## 6. Reference list

Bacchi, B., G. Grossi, R. Ranzi, and A. Buzzi, 2002: On the use of coupled mesoscale meteorological and hydrological models for flood forecasting in midsize mountain catchments: operational experience and verification, *Proc. of the 2nd International Symposium on Flood Defence*, Beijing, China, September 10-13, 2002, ed. by Wu et al., Science Press, New York Ltd., ISBN 1-880732-54-0, Vol II, 965-972.

Bacchi, B. and Ranzi, R., 2003: Hydrological and meteorological aspects of floods in the Alps: an overview. *Hydrol. Earth. System Sci.*, 7(6), 785-798.

- Becchi, I., Caporali, E., Castellani, L. and Palmisano, E., 1995: Hydrological control of flooding: Tuscany, October 1992, *Surveys in Geophysics*, **16**, 227-252.
- Bertò, A., A. Buzzi, and D. Zardi: 2004, 'Studio della perturbazione meteorologica responsabile della piena dell'Adige nel 1966 mediante analisi di traiettorie lagrangiane'. *Proc. XXIX Convegno Nazionale di Idraulica e Costruzioni Idrauliche*, Trento, 7-10 Sept. 2004, **2**, 227-234.
- Bertò, A., A. Buzzi and D. Zardi, 2005: A warm conveyor belt mechanism accompanying extreme precipitation events over north-eastern Italy. Proceedings of the 28th ICAM, The annual Scientific MAP Meeting, 2005, Zadar, Extended Abstracts, *Hrv. Meteorol. Casopis (Croatian Meteorological Journal)*, **40**, 338-341.
- Billet, S., and E.F. Toro, 1997: On WAF-type schemes for multidimensional hyperbolic conservation laws. *J. Comput. Phys.*, **130**, 1-24.
- Bougeault, P., and P. Lacarrere, 1989: Parameterisation of orography-induced turbulence in a mesoscale model. *Mon. Wea. Rev.*, **117**, 1872-1890.
- Browning K. A. and N. Roberts, 1994: Structure of a frontal cyclone. *Quart. J. Roy. Meteor. Soc.*, **120**, 1535-1557.
- Buzzi, A., 2005: Heavy precipitation and Alpine orography. Proc. of International Workshop on Timely Warnings of Heavy Precipitation Episodes and Flash Floods. Slovenian Meteorological Society, Ljubljana, 21-22 Oct. 2004, 9-15.
- Buzzi, A., M. Fantini, P. Malguzzi and F. Nerozzi, 1994: Validation of a limited area model in cases of Mediterranean cyclogenesis: surface fields and precipitation scores. *Meteorol. Atmos. Phys.*, **53**, 137-153.
- Buzzi, A., and L. Foschini, 2000: Mesoscale meteorological features associated with heavy precipitation in the southern alpine region. *Meteorol. Atmos. Phys.*, **72**, 131-146.
- De Angelis G., 1969: *Le acque dell'Arno*, Editrice Itinerari Lanciano.
- De Zolt, S., P. Lionello, P. Malguzzi, A. Nuhu, and A. Tomasin, 2006: The effect of the boundary conditions on the simulation of the 4 November 1966 storm over Italy. *Advances in Geosciences*, **7**, 199-204.
- Deardorff, J. W., 1980: Stratocumulus-capped mixed layers derived from a three dimensional model. *Boundary Layer Meteorol.*, **18**, 495-527.
- Drofa, O. V., and P. Malguzzi, 2004: Parameterisation of microphysical processes in a non-hydrostatic prediction model. Proc. 14<sup>th</sup> Intern. Conf. on Clouds and Precipitation (ICCP). Bologna, 19-23 July 2004, 1297-3000.
- Fea, G., A. Gazzola and A. Cicala, 1968: Prima documentazione generale della situazione meteorologica relativa alla grande alluvione del novembre 1966. CNR-CENFAM PV. **32**, 215 pp.

- Gouweleeuw, B., P. Reggiani, and A. De Roo, 2004: A European Flood Forecasting System EFFS. Full report of the EFFS project, funded under the FPV research programme of the European Commission. Available from A. De Roo, IES/JRC, Via E Fermi, TP261, 21020 Ispra, Italy, 304 pp.
- Grossi, G, Kouwen, N., 2004: Intercomparison among hydrologic simulations coupled to meteorological predictions provided by different mesoscale meteorological models, *Atti del XXIX Convegno di Idraulica e Costruzioni Idrauliche*, Trento, 7-10 Sept. 2004, Editorial Bios, **2**, 265-271.
- Kain, J.S., 2004: The Kain-Fritsch convective parameterisation: an update. *J. App. Meteorol.*, **43**, 170-181.
- Kain, J. S. and Fritsch, J. M., 1990: A one-dimensional entraining/detraining plume model and its application in convective parameterisation. *J. Atmos. Sci.*, **47**, 2784-2802.
- Meneguzzo, F., M. Pasqui, G. Menduni, G. Messeri, B. Gozzini, D. Grifoni, M. Rossi, G. Maracchi, 2004: Sensitivity of meteorological high-resolution numerical simulations of the biggest floods occurred over the Arno river basin, Italy, in the 20th century. *J. Hydrology*, **288**, 37-56.
- Ministero dei Lavori Pubblici, Servizio Idrografico, *Annali Idrologici – 1966* –Bologna, Parma, Pisa, Roma, Venezia, Istituto Poligrafico dello Stato, 1970.
- Mlawer, E.J., S.J. Taubman, P.D. Brown, M.J. Iacono, and S.A. Clough, 1997: Radiative transfer for inhomogeneous atmospheres: RRTM, a validated correlated-k model for the longwave. *J. Geophys. Res.*, 102D, **16**, 663-682.
- Morcrette, J.-J., 1991: Radiation and cloud radiative properties in the ECMWF operational weather forecast model. *J. Geophys. Res.*, **96D**, 9121-9132.
- Natale, L. and E. Todini, 1977: A constrained parameter estimation technique for linear models in hydrology, in *Mathematical Models for Surface Water Hydrology*, edited by T.A. Ciriani, U. Maione, J.R. Wallis, John Wiley & sons, 109-147.
- Orlandini, S., and R. Rosso, 1998: Parameterisation of stream channel geometry in the distributed modelling of catchment dynamics. *Water Resources Research*, **34** (8), 1971-1985.
- Ralph, F. M., P. J. Neiman and G. A. Wick, 2004: Satellite and CALJET aircraft observations of atmospheric rivers over the eastern North Pacific Ocean during the winter of 1997/98. *Mon. Wea. Rev.*, **132**, 1721-1745.
- Ranzi, R., M. Bochicchio, and B. Bacchi, 2002: Effects on floods of recent forestation and urbanisation in the Mella River (Italian Alps). *Hydrology and Earth System Sci.*, **6**(2), 239-265.
- Ranzi, R., Bacchi, B., and G. Grossi, 2003: Runoff measurements and hydrological modelling for the estimation of rainfall volumes in an alpine basin, *Quart. J. Roy. Meteorol. Soc.*, **129**, 653-672.
- Ranzi R., R. Buizza, A. Buzzi and P. Malguzzi, 2004: Previsione e controllo di eventi idrologici estremi: l'alluvione del novembre 1966 nel Triveneto, *Proc. XXIX Convegno di Idraulica e Costruzioni Idrauliche*, Trento, 7-10 Sept. 2004, **3**, 859-866.

- Ritter, B., and J. F. Geleyn, 1992: A comprehensive radiation scheme for numerical weather prediction models with potential applications in climate simulations. *Mon. Wea. Rev.*, **120**, 303-325.
- Shultz, P., 1995: An explicit cloud physics parameterisation for operational numerical weather prediction. *Mon. Wea. Rev.*, **123**, 3331–3343.
- Simmons, A. J., 2001: Development of the ERA-40 data assimilation system. *ECMWF Re-analysis project report series*, **3**, 11-31.
- Simmons, A. J., and J. K. Gibson, 2000: The ERA-40 Project Plan. *ECMWF Re-analysis project report series*, **1**, 62 pp.
- Smith, R. B., Q. Jiang, M. G. Fearon, P. Tabary, M. Dorninger, J. D. Doyle and R. Benoit, 2003: Orographic precipitation and air mass transformation: An Alpine example. *Quart. J. Roy. Meteorol. Soc.*, **129**, 433-454.
- Soderman, D., Meneguzzo, F., Gozzini, B., Grifoni, D., Messeri, G., Rossi, M., Montagnani, S., Pasqui, M., Orlandi, A., Ortolani, A., Todini, E., Menduni, G., Levizzani, V., 2003. Very high resolution precipitation forecasting on low cost high performance computer systems in support of hydrological modelling. Proceedings of the 17th Conference on Hydrology, AMS Annual Meeting (9–13 February 2003), available at: <http://www.ametsoc.org/AMS> or directly at: <http://ams.confex.com/ams/pdfview.cgi?username 55206>.
- Uppala, S., 2001: ECMWF Re-analysis 1957-2001, ERA-40. *ECMWF Re-analysis project report series*, **3**, 1-11.
- Uppala, S.M., P.W.Källberg, A.J.Simmons, U. Andrae, V.da Costa Bechtold, M. Fiorino, J.K.Gibson, J. Haseler, A. Hernandez, G.A. Kelly, X. Li, K. Onogi, S. Saarinen, N. Sokka, R.P. Allan, E. Andersson, K. Arpe, M.A. Balmaseda, A.C.M. Beljaars, L. van de Berg, J. Bidlot, N. Bormann, S. Caires, F. Chevallier, A. Dethof, M. Dragosavac, M. Fisher, M. Fuentes, S. Hagemann, E. Hólm, B.J. Hoskins, L. Isaksen, P.A.E.M. Janssen, R. Jenne, A.P. McNally, J.-F. Mahfouf, J.-J. Morcrette, N.A. Rayner, R.W. Saunders, P. Simon, A. Sterl, K.E. Trenberth, A. Untch, D. Vasiljevic, P. Viterbo, and J. Woollen, 2005: The ERA-40 Reanalysis. *Quart. J. Roy. Meteorol. Soc.*, **131**, 2961-3012.
- U.S. Department of Agriculture, Natural Resources Conservation Service, 1986: *Urban Hydrology for Small watersheds*, Technical Release 55.
- Warner, T., H.-M. Hsu, 2000: Nested-model simulation of moist convection: the impact of coarse-grid parameterized convection on fine-grid resolved convection. *Mon. Wea. Rev.*, **128**, 2211, 2231.
- Zampieri, M., 2004: Comparison among first, second and third order CBL model. *The 6<sup>th</sup> Symposium on Boundary Layers and Turbulence*. Portland, ME.
- Zhu, Y., and R. E. Newell, 1998: A proposed algorithm for moisture fluxes from atmospheric rivers. *Mon. Wea. Rev.*, **126**, 725-735.